Electron Hole Generation and Propagation in an Inhomogeneous Collisionless Plasma

F. Califano[1,2] and M. Lontano[1]
[1]*Istituto di Fisica del Plasma, EURATOM-ENEA-CNR, Italy*
[2]*Physics Department, University of Pisa, Italy*
(Received 24 May 2005; published 5 December 2005)

The generation of ''trains'' of electron holes in phase space due to an external electrostatic disturbance is investigated by using a Vlasov-Ampere code with open boundary conditions. Electron holes are produced mostly during the initial phase of the wave-plasma interaction, with a given drift velocity which is maintained until they exit the integration box, even in the presence of plasma inhomogeneities. They present macroscopic features, a dipolar electrostatic field and an electron density perturbation, which can be exploited for diagnostic purposes. Their equilibrium is intrinsically kinetic, in that they are accompanied by a stationary hole in the electron distribution function.

DOI: 10.1103/PhysRevLett.95.245002 PACS numbers: 52.65.Ff, 52.35.Fp, 52.35.Mw, 52.35.Sb

Among several physical processes accompanying the wave-plasma interaction, particular interest has been devoted to electron and ion holes in phase space [1–5], which are typical nonlinear kinetic structures producing macroscopic measurable effects in space plasmas [6–9]. The use of kinetic codes makes it possible to investigate at once both the hydrodynamic and the kinetic aspects of the wave-plasma interaction [10–15]. Kinetic codes have been recently used to describe holes in the particle distribution functions and the interaction of electron and ion holes in phase space [4,16–18].

In this Letter we present the results of kinetic investigations of the generation of electron holes (EHs) in electron phase space during the interaction of finite amplitude electrostatic (ES) disturbances with a collisionless electron-ion plasma. A Vlasov-Maxwell numerical code, based on the splitting scheme coupled to the third order accurate Van Leer interpolation scheme [19], has been implemented with open boundary conditions. We show how a series of drifting EHs is produced during the early phase of the external excitation of an ES wave packet in the plasma and how stable they are during the entire time of transit across the simulation box. Such EH's are produced well inside the plasma, for a sufficiently large pump field, during the breaking of the externally excited ES wave. We also show that they are produced and propagate independently of any plasma density gradient, even in regions which are forbidden to linear plasma waves. They are the result of a dynamical equilibrium among the density cavity associated with a hole in the electron phase space, a dipole ES field, and a gradient of electron pressure. If they move slowly enough, a slight ion density bump accompanies the EHs. The EH generation mechanism combined with the plasma inhomogeneity allows to isolate the solitary waves from the fluctuating background electric field, suggesting favorable experimental conditions for their observation.

We consider an unmagnetized 1D plasma in the region $0 < x < L_x$ described by the Vlasov equations:

$$\frac{\partial f_a}{\partial t} + v\frac{\partial f_a}{\partial x} + [\delta_a(E + E_{\rm dr}) + F_a]\frac{\partial f_a}{\partial v} = 0, \qquad a = e, i \tag{1}$$

where all quantities have been normalized to m_e, ω_{pe}, $\lambda_{\rm De}$, v_{te} and the electric field to $m_e v_{te}\omega_{pe}/e$. Furthermore, $\delta_e = -1$, $\delta_i = m_e/m_i = 1/1836$, $r_T = T_e/T_i = 1$. A nonuniform equilibrium is accomplished by introducing stationary *fictitious forces* acting on both plasma species: $F_e = d(\ln n_{e0})/dx$ and $F_i = (\delta_i/r_T) \times d(\ln n_{i0})/dx$. The self-consistent ES field $E(x, t)$ is calculated by means of the Ampere equation. The Poisson equation is used at the end of the simulation as a check of the ES field. The initial conditions are $E(x, t = 0) = 0$ with Maxwellian electrons and ions, each with temperature T_a. At the left boundary $x = 0$ we apply an external pump $E_{\rm dr}(0 \le x < \ell_{\rm dr}, t) = a_0 g(t)\sin(\omega_0 t)$, where $g(t) = \exp(-t^2/2\tau^2)$ models a finite duration ES disturbance, ω_0, τ, and a_0 are the frequency, the time duration, and the amplitude of the driver. The forcing has a Gaussian spatial profile and it is applied on a few grid points over one Debye length maximum, i.e., $\ell_{\rm dr} \le 1$. The equilibrium densities have been chosen in the form $n_{e0}(x) = n_{i0}(x) = 1 + \Delta n\{1 + \tanh[(x - x_m)/L_n]\}$, where the density is normalized to the unperturbed electron density at $x = 0$, $|2\Delta n|$ is the total density jump and L_n is the density scale length. At $x = x_c$ the electron density equals the critical density at the frequency ω_0, $n_c = m_e\omega_0^2/(4\pi e^2)$. The dimensionless forms of the equilibrium forces acting on the electrons and ions are $F_e(x) = (r_T/\epsilon)F_i(x) = \Delta n^2\,\mathrm{sech}^2[(x - x_m)/L_n]/\{1 + \Delta n[1 + \tanh((x - x_m)/L_n)]\}$. In all simulations, $x_m = 500$ has been considered. A number of simulations with different values of L_x, L_n, and x_c show that our results are independent of the boundary conditions. We also checked different spatial profiles for the driver $E_{\rm dr}$, still with $\ell_{\rm dr} \le 1$, and observed a very similar response of the plasma. Small amplitude forcing gives rise to the excitation of an ES wave packet, which propagates with the group velocity,

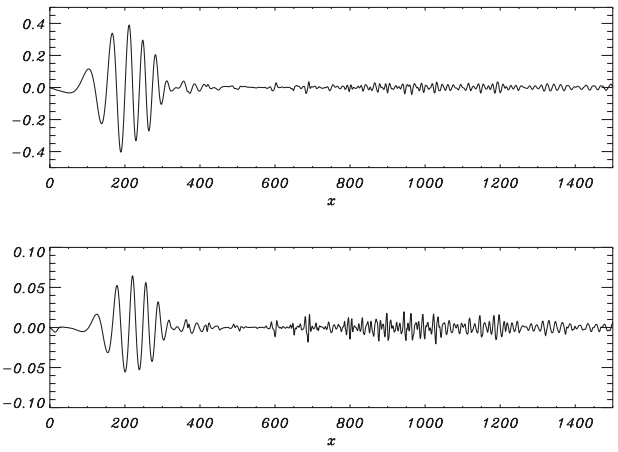

FIG. 1. The electric field E (upper frame) and the electron density fluctuations δn_e (lower frame) vs x at $t = 400$ with $\omega_0 = 1.1$, $a_0 = 10$, $\tau = 300$, $\Delta n = 0.4$, $L_n = 10$.

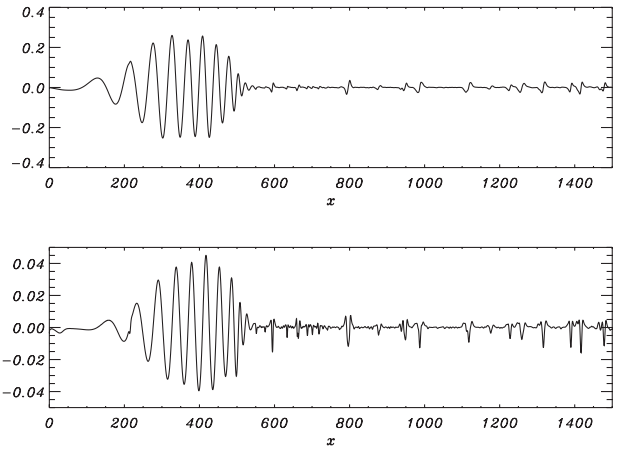

FIG. 3. The electric field E (upper frame) and the electron density fluctuations δn_e (lower frame) vs x at $t = 720$ with $\omega_0 = 1.1$, $a_0 = 10$, $\tau = 300$, $\Delta n = -0.4$, $L_n = 10$.

v_g. In this regime no EH is observed. For $E_{\rm dr} > 1$, a ''train'' of small density holes is formed, propagating ahead of the main ES pulse at a constant velocity $v_{\rm EH}$. In Fig. 1 the spatial distributions of the electric field and of the electron density perturbation are shown at $t = 400$. The background density increases around $x_c = 500$. The ES wave packet propagates at $v_g \approx 0.72$ up to x_c where it is reflected, eventually forming a stationary-wave pattern in the region $0 < x < x_c$, and producing a stationary ion density cavity with $|\delta n_i| \approx 2 \times 10^{-2}$ For $x > 100$ a sequence of density holes appears, propagating undisturbed across the plasma inhomogeneity. Each hole is characterized by an electron density dip of 1–2% of the background density, with side ''walls,'' and by a quasistatic dipole outward pointing ES field. The typical scale of a hole is $10\lambda_{\rm De}$. Corresponding to the density dips there are remarkable holes in the electron distribution function (EDF), centered around the $v_{\rm EH}$ of each hole. In Fig. 2 the phase space is shown for the same case as in Fig. 1. A hole in the EDF is present in correspondence of each density dip. The $v_{\rm EH}$ of each hole depends on its position on the velocity axis. The wave packet at $x < x_c$ behaves as a pure ES oscillation. Around the phase velocity $v_\phi \approx 4.2$ electron acceleration takes place. The EHs are usually situated at a velocity much lower than v_ϕ, varying from a fraction of v_{te} up to $2v_{te}$. In Fig. 3 the same plots as in Fig. 1 are shown for a decreasing background density, at $t = 720$. Shorter wavelengths are excited in the decreasing density region $450 < x < 550$, until the wave packet is strongly absorbed. However, the density holes slowly propagate undisturbed through the density gradient. In Fig. 4 E is plotted as function of t for the parameters of Fig. 3. A striking similarity with the features of the measured electric field, as shown in Figs. 1–3 in Ref. [20] is observed. In Fig. 5 the contributions to the force balance leading to the EH around $x \approx 800$ in Figs. 3 and 4, are shown. δn_e is plotted in the upper frame, E and $-n_e^{-1}(dp_e/dx)$ in the central frame, and δp_e and δT_e in the lower frame, respectively. In the density hole T_e increases enough to produce a pressure gradient which opposes to the ES force. We notice that the equilibrium is such that both T_e and p_e increase where

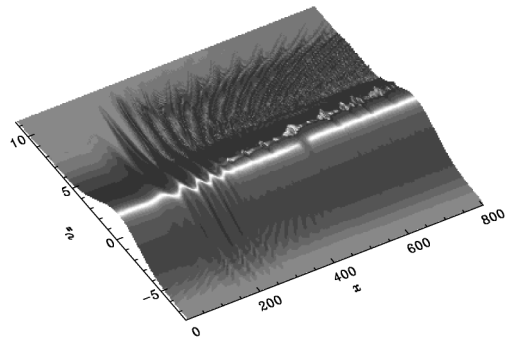

FIG. 2. The shaded isocontours of the EDF in the phase space (x, v_x) at $t = 400$, for an increasing density plasma. Parameters are the same as in Fig. 1.

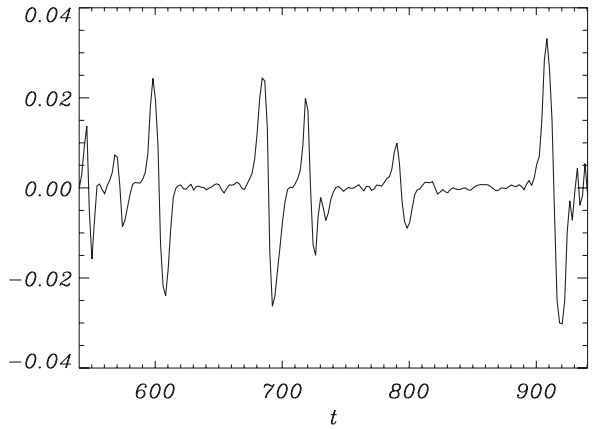

FIG. 4. The electric field E vs time, at $x = 750$. Parameters are the same as in Fig. 3.

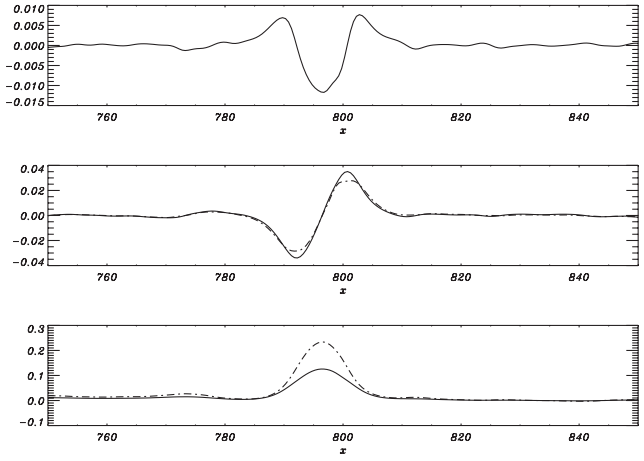

FIG. 5. δn_e (upper frame) E (solid line) and minus the electron pressure gradient over electron density, $-(1/n_e)dp_e/dx$ (dashed line); (central frame) the pressure fluctuations δp_e (solid line) and the electron temperature fluctuations δT_e (dot-dashed line); (lower frame) at $t = 720$. Parameters are the same as in Fig. 3.

electrons are expelled. The inward pointing electric force acting on electrons is almost completely balanced by the outward thermal force. In Fig. 6 the shaded isocontours of the EDF in the portion $750 \leq x \leq 850$, $-1.2 \leq v \leq 2.4$ of the phase plane is reported showing the details of the EH centered at $x \approx 800$. The whole set of holes moves at a differential velocity, early holes moving faster than ''newer'' holes, since the latter are generated along the velocity axis, closer to the thermal region than the former. Two subsequent times of the same run are shown in Fig. 7. The v_{EH} of the highlighted structure is about $0.28v_{te}$. They are slow enough to perturb the ion fluid as well, as shown in the lower frame where an ion density perturbation, in the form of a small amplitude bump, accompanies the structure. From inspection of Fig. 7 we can infer the coordinate where the considered EH was born. Since the drift velocity is strictly constant, the EH which has reached $x \approx 725$ at $t = 1200$, and $x \approx 810$ at $t = 1500$, has started its travel around $x \approx 390$, which is close to the maximum amplitude of the wave packet, before the density gradients (see Fig. 3). Most of earlier produced EHs are born mainly in

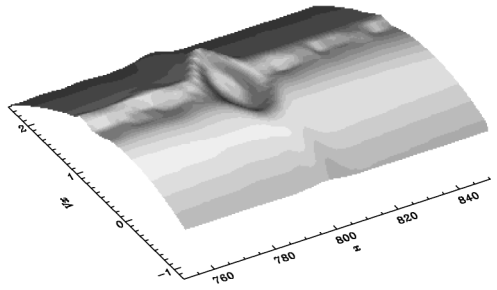

FIG. 6. The shaded isocontours of the EDF in the phase space (x, v_x) at $t = 720$. Parameters are the same as in Fig. 3.

the interval $100 < x < 300$. From the one-dimensional cold ion fluid equations, written in the reference frame moving at constant velocity $U = v_{\mathrm{EH}}$, the ion density perturbation $\delta n_i = n_i - n_\infty$, and the ion fluid velocity are easily calculated in the form $\delta n_i/n_\infty = (1 - 2e\phi/m_iU^2)^{-1/2} - 1$, $v_i(\xi) = [1 - (1 - 2e\phi/m_iU^2)^{1/2}]U$, where n_i, v_i, ϕ are the ion density, the ion fluid velocity, and the ES potential, respectively, and n_∞ is the unperturbed ion density. A bell-shaped potential, from which the dipolar electric field can be obtained, produces a bell-shaped ion density. As expected, the slower the structure the more pronounced the ion density perturbation is. In the frame of a one-dimensional fluid model for a drifting potential perturbation, an equation of state of the form $p_e = n_eT_e \propto n_e^{-\alpha}$, with $\alpha > 0$, can account for the existence of electron temperature and pressure maxima in correspondence of an electron density depression, induced by a bell-shaped ES potential. However, it does not explain the presence of walls around the electron density hole, an effect which is due to the kinetic nature of EHs. The electron induced electric field drag on the ions has been verified numerically by imposing a time independent dipolar electric field in the Vlasov equations. For velocities $\leq v_{te}$, we have reproduced the formation of the coupled electron dips and ion bumps, as well as their propagation at constant velocity. We have performed runs at higher frequency and stronger driving field, as, for example, the one reported in Fig. 8 where we plot E, δn_e, and δT_e vs x at $t = 600$ for $\Delta n = 0.4$. Again, regular oscillations in the wave packet at a level of $E \approx 0.1$ are established with density perturbations comparable with that of the main wave packet, and drift velocities in the range of $v_{te} - 2v_{te}$.

In this work we have investigated the excitation of EHs as a consequence of the interaction of an external ES disturbance of large amplitude with a background collisionless electron-ion plasma. These EHs appear either as ''precursors,'' propagating through the plasma with

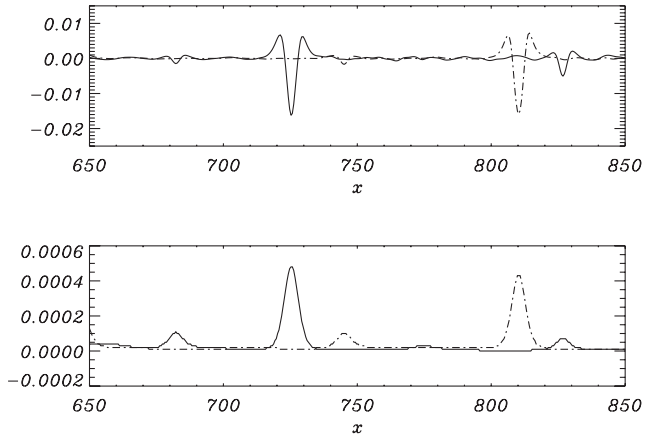

FIG. 7. The electron (upper frame) and proton (lower frame) density perturbations at $t = 1200$ (solid lines) and $t = 1500$ (dot-dashed line). Parameters are the same as in Fig. 3.

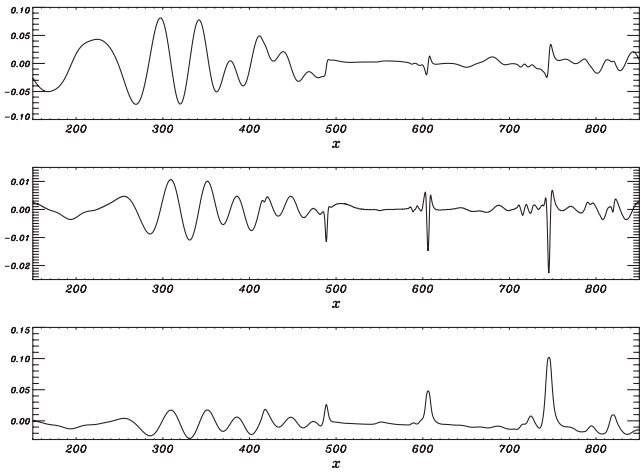

FIG. 8. E, δn_e, and δT_e (upper, central, and lower frames) vs x at $t = 600$ with $\omega_0 = 1.3$, $a_0 = 50$, $\tau = 300$, $\Delta n = 0.4$, $L_n = 10$.

$v_{\mathrm{EH}} > v_g$ (from a fraction to a few v_{te}) of linear ES waves, or they are continuously produced during the wave packet life. The EHs are not directly generated by the external forcing; indeed, they do form relatively far ($x \approx 100$) from the left boundary, however well before the plasma inhomogeneous region. In the presence of plasma inhomogeneities, the EHs exist in linearly nonaccessible regions for plasma waves, as well as in regions where they are strongly Landau damped. These ES solitary waves have an intrinsically kinetic nature, although they manifest macroscopic features as well, like a single-cycle ES field and a depleted electron density. According to our results, a plasma density gradient, both positive and negative, can be usefully exploited in order to ''separate'' the EHs from the ''parent'' ES wave, in order to observe the EHs features alone (electron density hole, dipolar electric field, local electron heating). This could be a practical method to be implemented in a laboratory experiment. Their characteristic scale ($\approx 10\lambda_{\mathrm{De}}$) agrees with the observations. As it is seen in Figs. 1, 3, and 8 (upper plots), the amplitude of the excited ES wave packet is smaller than that of the forcing field (applied at $x = 0$). The actual value of E is consistently determined by the plasma itself. According to the model developed by Coffey [21], the wave breaking field in a thermal plasma E_{wb} can be estimated. For $\omega_0 = 1.1$, $v_\phi \approx 4.2$ we find $E_{wb} \approx 0.99$; for $\omega_0 = 1.3$, $v_\phi \approx 1.77$ we get $E_{wb} \approx 0.0023$. The former value is an acceptable estimate of the field found for $\omega_0 = 1.1$. The second value is definitely much lower than that found for $\omega_0 = 1.3$. The discrepancy can be due to the water-bag model for the EDF used in [21]. After switching on ''adiabatically'' the external forcing, when the maximum allowed amplitude is achieved, wave breaking occurs, which self-regulate the electric field amplitude inside the plasma (which usually remains lower than unity). As a result of the wave breaking, the wave energy in excess, which will not go into the lower amplitude wave packet, is transformed into kinetic energy of accelerated electrons. At the same time, in the region $100 < x < 300$, electron holes are produced at velocities much lower than the wave phase velocity. Usually, ion density is not perturbed because EHs are relatively fast, on ion time scales. However, when $v_{\mathrm{EH}} < v_{te}$ a small bump in the ion density is observed. Other authors have considered the excitation of EHs in plasmas using kinetic codes either by ''... enlarging the hole in phase space artificially ...'' for $t < 0$ [16], or starting from an equilibrium plasma carrying a huge current, with the electron (ion) drift velocity being equal to the electron (ion) thermal speed [17]. We believe that our results can be considered more general, EHs being generated in a static equilibrium plasma subject to an external large amplitude drive. We observe their copious formation and demonstrate their high stability with respect to plasma inhomogeneities and their persistence for times long compared with other linear and nonlinear electron and also ion time scales.

This work was supported by the INFM Parallel Computing Initiative. Part of the work of F. C. is supported by the Istituto di Fisica del Plasma of Milan.

[1] H. Schamel, Plasma Phys. **14**, 905 (1972).
[2] H. Schamel, Phys. Plasmas **7**, 4831 (2000).
[3] G. Vetoulis *et al.*, Phys. Rev. Lett. **86**, 1235 (2001).
[4] B. Eliasson *et al.*, Phys. Rev. Lett. **92**, 095006 (2004).
[5] B. Eliasson *et al.*, Nonlinear Process. Geophys. **12**, 269 (2005).
[6] M. Temerin *et al.*, Phys. Rev. Lett. **48**, 1175 (1982).
[7] R. E. Ergun *et al.*, Geophys. Res. Lett. **25**, 2041 (1998).
[8] R. E. Ergun *et al.*, Phys. Rev. Lett. **81**, 826 (1998).
[9] R. E. Ergun *et al.*, J. Geophys. Res. **109**, A12220 (2004).
[10] A. Ghizzo *et al.*, Phys. Fluids **31**, 72 (1988).
[11] F. Califano *et al.*, Phys. Rev. Lett. **83**, 96 (1999).
[12] M. Lontano *et al.*, Phys. Rev. E **61**, 4336 (2000).
[13] M. V. Goldman *et al.*, Nonlinear Process. Geophys. **10**, 37 (2003).
[14] F. Califano *et al.*, Phys. Rev. E **67**, 056401 (2003).
[15] M. Lontano and F. Califano, Europhys. Conf. Abstr. **28G**, 1.062 (2004).
[16] K. Saeki *et al.*, Phys. Rev. Lett. **80**, 1224 (1998).
[17] D. L. Newman *et al.*, Phys. Rev. Lett. **87**, 255001 (2001).
[18] N. J. Sircombe *et al.*, Phys. Plasmas **12**, 012303 (2005).
[19] A. Mangeney *et al.*, J. Comput. Phys. **179**, 495 (2002).
[20] H. Matsumoto *et al.*, Geophys. Res. Lett. **30**, 1326 (2003).
[21] T. P. Coffey, Phys. Fluids **14**, 1402 (1971).